Theor Chem Acc (2016) 135:222
DOI 10.1007/s00214-016-1978-6

REGULAR ARTICLE

A theoretical study on the spectroscopy, structure, and stability of C_2H_3NS molecules

Marcin Gronowski[1] · Michał Turowski[1] · Thomas Custer[1] · Robert Kołos[1]

Received: 30 June 2016 / Accepted: 28 July 2016 / Published online: 16 August 2016

Abstract Here we report the results of a theoretical study devoted to the family of methyl thiocyanate (CH_3–SCN) isomers. From among 14 species sharing the C_2H_3NS stoichiometry, the most thermodynamically stable of these are methyl isothiocyanate (CH_3–NCS), methyl thiocyanate (CH_3–SCN), and mercaptoacetonitrile (HS–CH_2–CN). Energies were reliably predicted using the CCSD(T) variant of coupled-cluster calculations making use of a quadruple zeta-quality basis set. Minor contributions to the total energy, including scalar relativistic effects and extrapolation to the complete basis set limit, were obtained using second-order many-body perturbation theory. The three most stable isomers feature similar energy values (differing by few kJ/mol) that are much lower than those of the remaining C_2H_3NS species (more than 85 kJ/mol). Spectroscopic properties including rotational constants, anharmonic vibrational frequencies, infrared absorption intensities (harmonic), Raman activities, and the energies of excited electronic states have been derived using coupled-cluster or density functional theory for the whole set of C_2H_3NS molecules. Additionally, infrared absorption intensities and frequencies of overtone and combination bands are given for the three lowest energy isomers.

Keywords Thiocyanate · Spectroscopy · Ab initio · Isomers · Stability · Electronic states

Electronic supplementary material The online version of this article (doi:10.1007/s00214-016-1978-6) contains supplementary material, which is available to authorized users.

✉ Marcin Gronowski
marcingronowski@gmail.com

[1] Institute of Physical Chemistry, Polish Academy of Sciences, 44/52 Kasprzaka, 01-224 Warsaw, Poland

1 Introduction

The astrochemistry of small, unsaturated molecules containing nitrogen, carbon, and sulfur is poorly understood. This observation applies, in particular, to the family of compounds containing the –NCS functional group which include species like isothiocyanic acid (HNCS) and thiocyanic acid (HSCN). Both have been detected in the interstellar medium (ISM) [1–4], and their astrochemical formation pathways recently proposed [2, 5]. These are the only such molecules detected in the interstellar medium which contain an atom each of carbon, sulfur, and nitrogen. Four-atomic [C, H, N, S] isomers have already been studied on theoretical and experimental grounds [6–8] and HNCS turns out to be the most stable among them with the HSCN molecule only 6.3 kcal/mol higher in energy. HCNS and HSNC arrangements may also be important, with energies only 34.4 and 36.0 kcal/mol higher than that of HNCS.

Many interstellar molecules like HCN, HNC, HC_3N, HC_5N, and SH_2 have methyl-bearing analogues which have also been observed in the interstellar medium. It is therefore likely that methyl-bearing molecules featuring the –NCS functionality can also be found, potentially along with some of their structural isomers. As little spectroscopic data exists for the majority of species in the C_2H_3NS family, more must be known about them before any search can be contemplated. To date, no C_2H_3NS family member has been detected in space.

Among C_2H_3NS species, methyl isothiocyanate (CH_3NCS) is perhaps the best known terrestrially. This is a volatile substance commonly used as a pesticide [9]. It easily reaches the atmosphere following application and photochemical processes contribute to its eventual decomposition and removal [10–12]. Although CH_3SCN and CH_3NCS are commercially available, their spectroscopy and photochemistry are poorly known. Electronic absorption spectra

are similar to those reported for HNCS [13, 14]. Gas-phase photolysis products include CH_3, NCS, and CN [15–20]. More decomposition products were reported for CH_3SCN subjected to electric discharges [21]. Recently, Møllendal and collaborators measured the gas-phase rotational spectroscopy of mercaptoacetonitrile, another isomer of C_2H_3NS stoichiometry [22]. From this study, we know that mercaptoacetonitrile has two conformers with a calculated energetic separation between them of 4.68 kJ/mol [22]. To the best of our knowledge, no experimental data are available for the isomerisation reactions of C_2H_3NS family members. Such processes are potentially important, for studies of photochemical reactions in solid noble gases.

Fu et al. [23] analyzed the potential energy surface (PES) of the [CH_3, N, C, S] system where the CH_3 group remained an indivisible unit during the calculations. Here we consider the [2C, 3H, N, S] PES where all atoms can take any position and predict the spectroscopic properties of the relevant bound species. Very few high-level quantum chemical studies on simple thiocyanates or isothiocynates have been reported. The most advanced was carried out in 1996 by Koput [24], who used the coupled-cluster approach with a triple-zeta basis set to derive the potential energy surface for the CNC bending motion in CH_3NCS and to predict its rotational energy levels. Rotational constants and geometric parameters of MeNCS were also reported by Palmer and Nelson [25].

The relatively large number of atoms in C_2H_3NS makes a search for all possible isomers based on chemical intuition impractical. To overcome this, Saunders [26] proposed a stochastic search method where an arbitrarily selected structure is first optimized and used as a starting point in the search for further isomers. The next arrangement can then be generated by a "kick" that slightly (and randomly) changes the positions of all atoms. Each kick is followed by geometry optimization. This iteratively repeated procedure, while simple and efficient, may fail when the energy minima are too far apart (as is likely in our case). Therefore, an alternative approach was applied here, based on randomly chosen atomic configurations [27, 28].

2 Theoretical methods

2.1 General procedure

A procedure similar to that implemented here in the search for all possible energy minima on the potential energy surface (PES) has been described previously [28]. Starting structures were repeatedly generated as random arrangements of atoms placed at the nodes of a grid (spaced by 0.6 Å) inside a 6.5 × 6.5 × 6.5 Å rectangular box. Such initial atomic configurations were subjected to geometry optimization using density functional theory (DFT) at the B3LYP/4-31G** [29–33] level. Resultant structures were added to a database of bound species if they were different from any of those previously generated. Intermolecular complexes were not included in this database. The search procedure was terminated after completion of approximately 3000 optimization runs. At this number of runs, each structure had appeared at least twice. B3LYP/aug-cc-pVDZ [29, 34, 35] geometries were subsequently calculated for each molecule from this database. This second round of calculations allowed us to distinguish the most stable isomers with more certainty. The geometries predicted at this level are used as a starting point for a final round of very precise calculations providing final energies and spectroscopic constants.

A more detailed study of the most stable atomic arrangements (at the B3LYP/aug-cc-pVTZ level [29, 34, 35]) included geometry optimizations which were then followed by anharmonic calculations (VPT2 [36]) with numerical differentiation along normal modes. This supplied harmonic (ω_{B3LYP}) and anharmonic (ν_{B3LYP}) frequencies, as well as vibration–rotation coupling constants and quartic centrifugal distortion constants. Raman intensities and natural bond orbitals [37–39] (NBO) were also calculated at the same level of theory.

Next, coupled-cluster computations (CCSD [40–42] with the cc-pVTZ [34, 35] basis set) were performed to improve the precision of molecular geometry predictions. Equilibrium electric dipole moment values were obtained at the same level of theory. Consequently, geometry optimizations were carried out for the 12 most stable isomers with the CCSD(T) method (singles, doubles, and the perturbative treatment of triple excitations) in the frozen-core approximation. Harmonic vibrational frequencies $\omega_{CCSD(T)}$ were obtained using numerical second derivatives of the total energy with respect to nuclear positions.

Calculations at the B3LYP/aug-cc-pVDZ and CCSD/cc-pVTZ levels of theory were used to search for low-lying triplet electronic states for each of the C_2H_3NS isomers using singlet structures as starting points. Additional calculations searching for singlet excited states were performed in two steps. First, vertical excitation energies were calculated by EOM-CCSD/cc-pVTZ. Next, selected structures were optimized using CIS/aug-cc-pVDZ. These calculations are used to confirm that each molecule has a singlet ground state as well as to determine potential photochemical decomposition pathways.

The recommended vibrational frequencies were based on harmonic values obtained at the CCSD(T) level and on B3LYP-derived anharmonic corrections, as detailed elsewere [28, 43–46]. Similarly, our recommended ground-state geometric structures (and the rotational constants that depend on them) were based on both coupled-cluster and

DFT calculations [5, 27, 28, 45–48]. Vibration–rotation coupling constants were obtained at the VPT2-B3LYP/aug-cc-pVTZ level. The software package Gaussian 09 [49] was used in these computations for the whole set of isomers. The frozen-core approximation was used for all ab initio calculations.

2.2 The most stable isomers

The three lowest energy C_2H_3NS isomers were subjected to a more accurate theoretical treatment. Their molecular structures were derived at the CCSD(T)/cc-pVQZ level. The following formula, similar to that employed in our previous report [28], was used to obtain final energy values:

$$\begin{aligned} E = {} & E_{cc-pVQZ}^{corr,CCSD(T)} + \left(E_{CBS}^{corr,MP2} - E_{cc-pVQZ}^{corr,MP2}\right) \\ & + \left(E_{cc-pCVQZ}^{MVD2,MP2} + E_{aug-cc-pCVQZ}^{corr,MP2} - E_{cc-pVQZ}^{corr,MP2}\right) \\ & + \left(E_{cc-pVTZ}^{corr,CCSDT} - E_{cc-pVTZ}^{corr,CCSD(T)}\right) + E_{cc-pV5Z}^{total,HF} \\ & + E_{cc-pVQZ}^{DBOC,CCSD} + E_{cc-pVTZ}^{ZPE,CCSD(T)} \end{aligned} \quad (1)$$

The meanings of the sub- and superscripts in the energy terms $E_C^{A,B}$ are the following: A (energy type)—this can be any of the correlation (*corr*), total (*total*), diagonal Born–Oppenheimer correction (*DBOC*) [50], mass-velocity and Darwin term (*MVD2*) [51, 52], or zero-point energy (*ZPE*); B—method; C—basis set (*CBS* denotes the complete basis set). All contributions to the energy were calculated assuming the CCSD(T)/cc-pVQZ geometry, except for diagonal Born–Oppenheimer corrections $E_{cc-pVQZ}^{DBOC,CCSD}$ (CCSD/cc-pVQZ geometry) and zero-point energy values $E_{cc-pVTZ}^{ZPE,CCSD(T)}$ (CCSD(T)/cc-pVTZ geometry).

The $1/X^3$ error law [53, 54] (X denoting the basis set cardinal number) served to estimate the complete basis set (CBS) limits of correlation energy [53, 54] which is given by:

$$E_{CBS}^{corr,MP2} = E_{cc-pVQZ}^{corr,MP2} + \frac{125\left(E_{cc-pV5Z}^{corr,MP2} - E_{cc-pVQZ}^{corr,MP2}\right)}{61} \quad (2)$$

Anharmonic (VPT2) calculations, performed at the CCSD(T)/cc-pVTZ level, supplied the zero-point vibrational energy $\left(E_{cc-pVTZ}^{ZPE,CCSD(T)}\right)$ values, electric dipole moment for the ground vibrational states (μ_0), infrared absorption intensities of overtone and combination transitions, vibration–rotation coupling constants (α_i^A, α_i^B, α_i^C), and the rotational distortion constants. The software package CFOUR v.1 [55] was used in these computations for the three lowest energy isomers. The frozen-core approximation was not used in these computations. The estimation of room-temperature thermodynamic stabilities relied on partition functions obtained using B3LYP/aug-cc-pVTZ-derived anharmonic vibrational frequencies [56] and were carried out using the Gaussian 09 package [49].

3 Results and discussion

3.1 Stability of isomers

More than 100 species were found in course of preliminary studies using B3LYP/4-31G** and B3LYP/aug-cc-pVDZ calculations. From the list generated by these runs, we selected 45 of the most stable isomers for further CCSD/cc-pVTZ studies. From this set of 45, the 20 most stable isomers are presented in Fig. 1. Species, including thionitroso ethane [57], 1,3-didehydro-1-methyl-1*H*-1λ^4-thiazirine [23], 2-thia-4-azabicyclo[1.1.0]butane [58], and 2-methyl-3-thiaziridinylidene [23] are in the longer list but not included on Fig. 1, because they have high relative energies with respect to ***1***: 183, 204, 238, 282 kJ/mol, respectively.

Figure 1 presents the most stable C_2H_3NS isomers together with their corresponding (relative) energy values. Mean absolute errors of 65.1 and 10.5 kJ/mol have been reported [59] for the predictions of atomisation energies and reaction enthalpies, respectively, using all-electron correlation and CCSD/cc-pCVTZ. Considering these values and the results of our earlier CCSD/cc-pVTZ study on C_2HNS-stoichiometry molecules [28], we estimate the precision of our relative energy calculations to be better than 30 kJ/mol. This is sufficient to identify isomers ***1***, ***2***, and ***3*** as the most stable, but do not permit reliable prediction of the order of stability for the three lowest energy isomers.

Our most precise calculations (Table 1) reduced the energetic difference between ***1*** and ***3*** from 12.4 to 6.0 kJ/mol. Inclusion of thermal corrections at the VPT2-B3LYP/aug-cc-pVTZ level significantly changed the results. For standard (298.15 K, 1 bar) conditions and including thermal corrections, ***2*** becomes the most stable isomer, but energetic differences remain small (Table 1). It seems likely that the thermodynamic stability under normal conditions decreases in the flowing order with the first being the most stable: ***2***, ***1***, ***3***. However, the energetic differences between these isomers are low and of the same order of magnitude as the uncertainty of the calculation. The fact that ***1*** is among the three lowest energy chemicals seems to contradict what is known about the stability of molecules ***1***, ***2***, and ***3*** from reports where handling of the chemicals was described. The last two chemicals are commercially available and can be stored with no difficulty, unlike species ***1*** [60, 61]. The lower stability of ***1*** may be determined by other factors, such as the existence of a low energetic barrier to a thermally activated reaction or susceptibility to a photochemical transformation.

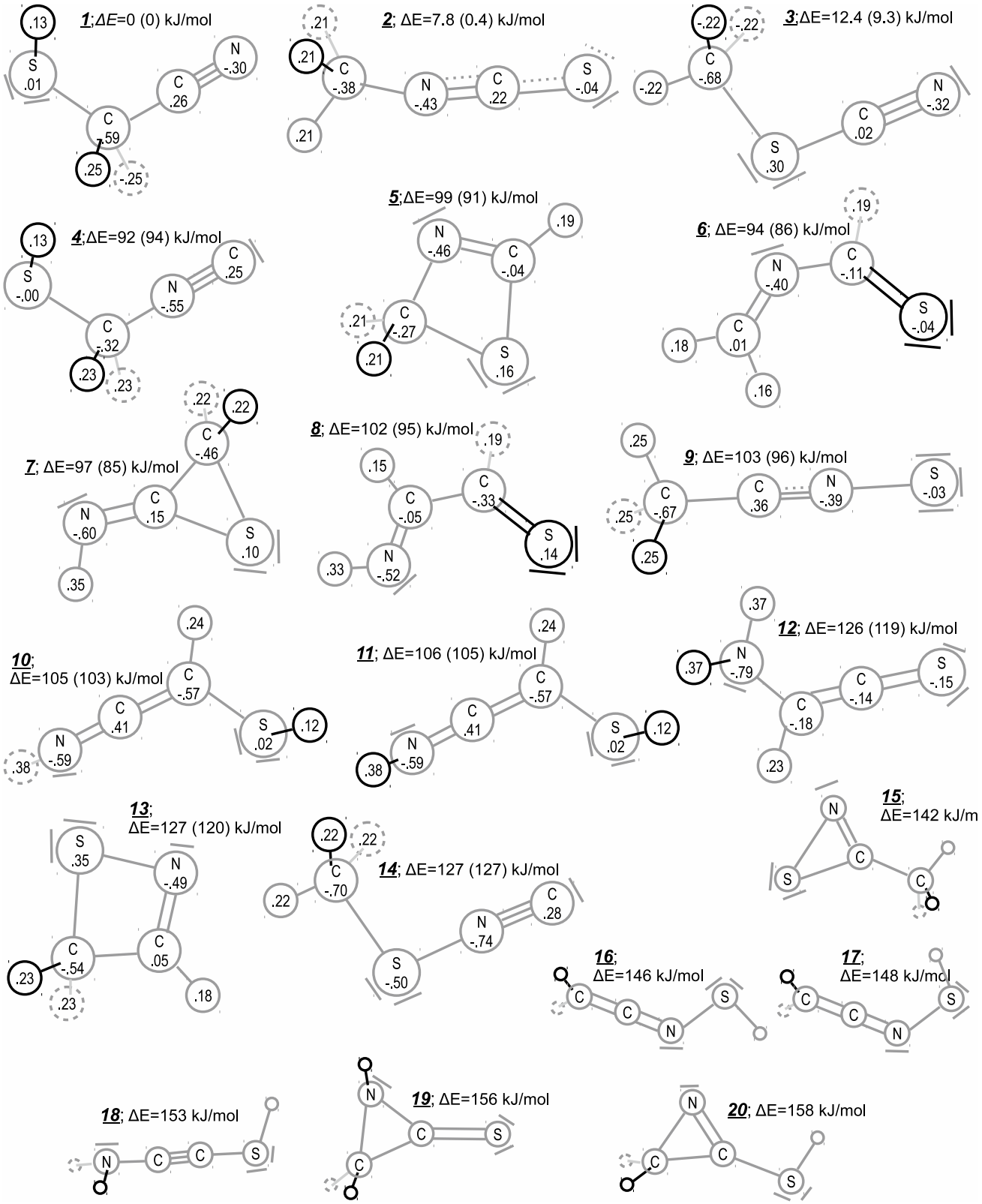

Fig. 1 Molecular structures corresponding to the lowest energy minima within a potential energy surface describing C_2H_3NS singlet species. Isomer labels are followed by ZPE-corrected CCSD/cc-pVTZ relative energies, calculated with respect to species ***1***. More precise CCSD(T)/cc-pVTZ relative energies are given in parentheses, when available. Atomic charges (for the first 14 isomers) and Lewis-type dash formulae are based on NBO analysis at the B3LYP/aug-cc-pVTZ level. Circles drawn with gray full lines, black full lines, and dashed gray lines represents the atoms situated, respectively, in the plane of the figure, in front of the plane or behind the plane

Table 1 Relative energies (ΔE) and relative standard Gibbs free energies ($\Delta G_{298.15K}$) for the three most stable C_2H_3NS stoichiometry molecules, together with energy terms of the Eqs. 1 and 2

	Unit	***1***	***2***	***3***
$E_{cc-pVQZ}^{corr,CCSD(T)}$	hartree	−0.937268	−0.941883	−0.940366
$E_{CBS}^{corr,MP2} - E_{cc-pVQZ}^{corr,MP2}$	hartree	−0.313280	−0.312709	−0.313513
$E_{cc-pCVQZ}^{MVD2,MP2} + E_{aug-cc-pCVQZ}^{corr,MP2} - E_{cc-pVQZ}^{corr,MP2}$	hartree	−1.58949	−1.58882	−1.58976
$E_{cc-pV5Z}^{total,HF}$	hartree	−529.527032	−529.526252	−529.522497
$E_{cc-pVQZ}^{DBOC,CCSD}$	hartree	0.011757	0.011755	0.011770
$E_{cc-pVTZ}^{ZPE,CCSD(T)}$	hartree	0.045035	0.047825	0.046380
ΔE	kJ/mol	0	0.5	6.0
$\Delta G_{298.15K}$	kJ/mol	0	−5.2	4.9

Table 2 Recommended equilibrium rotational constants and ground-state rotational constants of C_2H_3NS isomers computed using the hybrid CCSD(T) + B3LYP approach [5, 27, 28, 45–48] (see the text)

	A_e/GHz	B_e/GHz	C_e/GHz	A_0/GHz	B_0/GHz	C_0/GHz	μ_e/D	α/Bohr^3
1	23.08	3.107	2.826	22.94 (23.11)[a]	3.103 (3.105)[a]	2.813 (2.820)[a]	3.1	42.6
2	90.84 [83.53][b]	2.5409 [2.5385][b]	2.5111 [2.5024][b]	105.6 (81.07)[c]	2.511 (2.537)[c]	2.494 (2.499)[c]	4.2	49.5
3	15.61	4.164	3.358	15.60 (15.79)[c]	4.147 (4.155)[c]	3.340 (3.354)[c]	4.0	43.6
4	24.14	3.292	2.998	24.05	3.278	2.983	3.1	44.3
5	13.88	7.327	4.950	13.79	7.277	4.912	0.8	42.5
6	22.00	3.804	3.365	22.44	3.754	3.330	2.4	47.7
7	14.18	5.384	4.009	14.08	5.359	3.983	0.9	46.2
8	19.58	3.790	3.190	19.51	3.769	3.170	3.2	45.9
9	158.8	2.397	2.397	156.9	2.395	2.395	6.0	51.1
10	29.54	2.960	2.763	29.48	2.949	2.750	1.1	48.6
11	29.29	2.965	2.766	29.16	2.954	2.755	2.4	48.6
12	41.78	2.718	2.569	41.93	2.708	2.558	1.9	50.2
13	12.61	8.014	5.060	12.53	7.969	5.027	3.0	42.5
14	16.14	4.458	3.573	16.16	4.437	3.553	3.9	45.6

Equilibrium electric dipole moment and polarizability values derived using CCSD/cc-pVTZ are also given

[a] Experimental value [22]

[b] Based on CCSD(T) calculations of Ref. [25]

[c] Experimental value [62]

3.2 Spectroscopic properties of selected isomers

3.2.1 Rotational spectroscopy

Calculated rotational constants are collected in Table 2. Available experimental values, concerning the vibrationless states of species ***1***, ***2*** and ***3*** [22, 62, 63], allow estimation of the precision of these predictions. Absolute differences between experimental and theoretical values are 0.4 and 0.2 %, for C_0 and B_0 of ***3***, respectively. In the case of ***1***, corresponding values are even smaller, while for ***2***, these values are 0.2 and 1.0 %. A significant error observed for the predicted B_0 value of ***2*** may stem from the large amplitude of the low frequency vibration. In previous studies, employing the same theoretical approach, the absolute deviation from experimental B_0 and C_0 values varied between 0.05 and 0.6 % [5, 45]. Differences between equilibrium and ground-state rotational constants are on the order of 0.5 %. Electric dipole moments calculated for the most stable isomers fall in the range between 0.8 and 6 D. This should allow for microwave detection of at least some of these molecules.

3.2.2 Infrared spectroscopy

Tables 3, 4, 5 and 6 (see Online Resource for their full versions) collect information concerning the vibrational spectroscopy of molecules ***1***, ***2***, ***3***, and ***9*** for

Table 3 Vibrational spectroscopy of ***1***

	Frequency/cm^{-1}			IR intensity/km × mol^{-1}			Raman activ./$Å^4$ × AMU^{-1}
	Harmonic	Anharmonic		Harmonic		Anharmonic	Harmonic
	CCSD(T)	CCSD(T,fc) + B3LYP	CCSD(T)	CCSD,fc	CCSD(T)	CCSD(T)	B3LYP
Fundamental modes							
ν_1	3139	2988	2994	0.70	0.84	0.80	53
ν_2	3105	2981	2979	1.9	1.8	2.5	1.2×10^2
ν_3	2710	2583	2604	0.31	0.38	1.3	1.1×10^2
ν_4	2310	2255	2274	0.70	0.32	0.15	1.3×10^2
ν_5	1476	1441	1435	5.7	5.9	5.4	6.6
ν_6	1290	1254	1258	6.0	5.4	4.6	11
ν_7	1234	1195	1200	4.1	4.1	3.3	2.5
ν_8	1022	998	956	5.4	5.3	8.9×10^3	3.2
ν_9	953	921	931	4.9	4.2	3.0	1.5
ν_{10}	801	794	788	0.19	0.17	0.17	8.3
ν_{11}	714	694	704	4.6	4.5	1.9	16
ν_{12}	490	475	484	0.099	0.056	0.083	4.5
ν_{13}	369	350	364	0.69	0.85	0.55	1.2
ν_{14}	221	277	203	20	20	18	0.72
ν_{15}	175	195	171	6.9	6.3	7.5	2.4
Selected overtone and combination modes (intensities higher than 1 km × mol^{-1})							
$\nu_{12} + \nu_{14}$	712	752	684			3.1	
$\nu_{10} + \nu_{14}$	1023	1079	1038			4.7×10^3	
$\nu_5 + \nu_7$	2710	2632	2632			2.2	

which experimental values are also available. Additional data for less stable C_2H_3NS species are provided in the Online Resource. Focusing our attention on theoretical results alone, for the three lowest energy isomers, the vibrational frequencies predicted by hybrid CCSD(T) + VPT − B3LYP [28, 43–46] calculations and by the standard VPT2-CCSD(T) procedure can be compared. As reported previously [28, 43–46], the hybrid approach satisfactorily reproduces fundamental frequencies. For overtone and combination modes, the discrepancy between VPT2-CCSD(T) and hybrid methods is higher, especially in the case of low-energy vibrations. In spite of its slightly lower accuracy, CCSD(T) + VPT − B3LYP predictions are still sufficient for the identification of isomers by IR absorption spectroscopy. Isomers ***1*** and ***3*** feature rather low IR intensities, while for each of the following species: ***2***, ***4***, ***6***, ***7***, ***9***, ***10***, ***11***, ***12***, and ***14***, at least one intense (in excess of 100 km/mol) IR transition is to be expected. While our theoretical predictions already allow for a critical evaluation of some published spectral assignments concerning ***1***, ***2***, ***3***, and ***9***, the reliable identification of combination and overtone modes will require further, dedicated experimental studies.

Calculations can be compared to limited experimental data as well. No IR spectra have been measured for the isomers ***4***–***14***, with the exception of the cryogenic argon matrix-isolated species ***9*** [64]. We limit our discussion here to ***1***, ***2***, and ***3***. Mathias and Shimanski [61], after having synthesized compound ***1***, reported on its most prominent IR bands measured in the condensed phase. These bands are in acceptable agreement with our ab initio results. However, the complete IR spectrum of ***1*** was not given. Because of this, no experimental values are listed in Table 3. Our predictions suggest low intensities for each of the IR transitions of ***1***. The only exception is the anharmonic prediction for the ν_8 vibration, for which the intensity is surprisingly high in comparison with harmonic result. We identified a strong resonance between ν_8 and $\nu_{10} + \nu_{14}$ as the main contributor to this intensity increase. A reliable prediction of resonances is challenging, even at a high level of theory, so this anharmonic intensity may be significantly overestimated.

For ***2***, IR [65–68] and Raman [65] spectra have been measured. Gas-phase frequencies [68] of the fundamental modes match our present theoretical predictions fairly well (Table 4). More complicated is the case of overtone and combination modes, some of which were identified for gaseous- and condensed-phase samples [65, 66]. Our theoretical predictions deserve several comments:

1. As pointed out elsewhere [24], the internal rotation of a methyl group is a large-amplitude vibration that can-

Table 4 Vibrational spectroscopy of **2**

	Frequency/cm^{-1}				IR intensity/km × mol^{-1}			Raman activ./Å^4 × AMU^{-1}
	Harmonic	Anharmonic		Exp.[a]	Harmonic		Anharmonic	Harmonic
	CCSD(T)	CCSD(T,fc) +B3LYP	CCSD(T)		CCSD,fc	CCSD(T)	CCSD(T)	B3LYP
Fundamental modes								
ν_1 A″	3145	2993	2994	2966	8.1	9.7	1.1×10^1	1.1×10^1
ν_2 A′	3127	2983	2993	2966	8.6	1.0×10^1	9.9	1.1×10^1
ν_3 A′	3067	2944	2946	2952	43	4.6×10^1	1.9	3.8×10^1
ν_4 A′	2198	2078	2142	2083	1.2×10^3	1.1×10^2	5.0×10^2	1.1×10^1
ν_5 ″	1522	1487	1473	1421	7.8	7.6	6.5	8.6
ν_6 A′	1513	1476	1468	1421	7.6	6.8	5.2	6.9
ν_7 A′	1465	1446	1436	1425	7.3×10^1	7.2×10^1	6.3×10^1	28
ν_8 A′	1186	1148	1141	1181	1.9	6.5	1.3	7.6
ν_9 A′	1135	1114	1113	1108	0.15	0.12	1.9	0.049
ν_{10} A″	1133	1087	1110	1108	2.5×10^1	2.8×10^1	1.4×10^1	11
ν_{11} A′	683	666	662	680	3.7×10^1	1.9×10^1	2.1×10^1	13
ν_{12} A′	483	457	509	535	2.1×10^1	3.1×10^1	2.1×10^2	0.43
ν_{13} A″	464	447	460	417	2.0	1.2	0.91	0.041
ν_{14} A′	97	113	82	110	2.0×10^1	2.7×10^1	2.1×10^1	2.0
ν_{15} A″	15				3.2	2.4		0.74
Selected overtone and combination modes with IR intensities higher than 1 km × mol^{-1}								
$2\nu_{14}$	194	191	148				1.5	
$\nu_{12} + \nu_{14}$	580	560	584				4.0	
$\nu_8 + \nu_{14}$	1283	1246	1217				1.7	
$\nu_7 + \nu_{11}$	2148	2096	2097				2.3×10^1	
$\nu_6 + \nu_{11}$	2196	2142	2130				2.8×10^2	
$2\nu_{10}$	2267	2183	2221				1.5×10^2	
$2\nu_9$	2270	2225	2222				1.1	
$\nu_4 + \nu_{14}$	2295	2215	2242				1.4×10^2	
$\nu_8 + \nu_{10}$	2320	2234	2250				4.7×10^1	
$2\nu_8$	2373	2293	2278				8.3	
$\nu_4 + \nu_{12}$	2680	2563	2654				3.5	
$\nu_4 + \nu_{11}$	2881	2771	2815				1.9×10^1	
$2\nu_7$	2929	2853	2853				2.4	
$2\nu_6$	3026	2962	2933				2.1×10^1	
$2\nu_5$	3045	2984	2938				5.3×10^1	
$2\nu_4$	4395	4150	4235				5.6	

[a] Ref. [68], gas phase

not be treated using VPT2. With this in mind, we give no predictions regarding the ν_{15} anharmonicity or any parameters of related overtone or combination bands.

2. Interpretation of IR spectra in the 2000–2300 cm^{-1} region, where our ab initio calculations locate the fundamental band ν_4 ("antisymmetric" NCS stretching), is very challenging. The band $\nu_6 + \nu_{11}$ (CH_3 antisymmetric deformation coupled to the NCS "symmetric" stretching) should be a factor of two less intense than ν_4. In the same region one can also expect to find an overtone of a CH_3 twisting mode ($2\nu_{10}$), as well as the $\nu_4 + \nu_{14}$ combination (ν_{14} is the CNC bending), with their predicted intensities about two times lower than that of $\nu_6 + \nu_{11}$. An additional band in this region might come from $\nu_8 + \nu_{10}$ and $\nu_7 + \nu_{11}$ vibrational transitions. These are predicted to be 6 and 12 times less intense in IR than $\nu_6 + \nu_{11}$. Reliable spectral assignments of all combination bands will require further experimental studies and possibly the use of isotopologues.
3. The combination band $\nu_4 + \nu_{11}$, arising from NCS "antisymmetric" and "symmetric" stretches, is pre-

Table 5 Vibrational spectroscopy of ***3***

	Frequency/cm^{-1}					IR intensity/km × mol^{-1}			Raman activ./Å^4 × AMU^{-1}
	Harmonic	Anharmonic		Exp.		Harmonic		Anharmonic	Harmonic
	CCSD(T)	CCSD(T,fc) +B3LYP	CCSD(T)	Gas phase	Solid, Raman	CCSD,fc	CCSD(T)	CCSD(T)	B3LYP
Fundamental modes									
ν_1	3179	3029	3035	3033 [a,c]	3038	1.7	1.5	2.7	53
ν_2	3167	3020	3026	3014	3025	1.6	1.5	2.5	65
ν_3	3088	2970	2978	2951 [a, c]	2944, 2938	10	9.9	9.0	1.7×10^2
ν_4	2225	2173	2193	2171 [a,c]	2155	8.1	7.2	5.9	1.5×10^2
ν_5	1502	1465	1458	1435 [a,c]	1438, 1432	8.5	8.5	7.3	3.0
ν_6	1485	1435	1444		1424, 1415	7.5	7.7	7.0	5.2
ν_7	1366	1326	1337	1329 [a,c]	1318, 1309	5.5	5.1	0.083	1.1
ν_8	1007	985	989	991 [a,c]	1005, 996	7.5	7.4	6.9	0.87
ν_9	984	966	968	968 [a,c]	974	2.8	2.9	2.8	0.26
ν_{10}	722	700	705	709 [a,c]	703, 704	1.5	1.2	1.1	3.9
ν_{11}	682	666	674	692 [b,c]	678	0.61	0.34	0.39	19
ν_{12}	459	447	455		467	0.17	0.22	0.22	1.0
ν_{13}	411	389	405	440 [c]	421	3.0	2.4	2.3	0.57
ν_{14}	174	170	174	172 [a,c]	190	5.4	5.1	5.0	5.1
ν_{15}	161	157	147	131 [d]		0.032	0.028	0.019	0.092
Selected overtone and combination modes with IR intensities higher than 1 km × mol^{-1}									
$2\nu_{11}$	1364	1326	1340					8.6	
$2\nu_5$	3004	2899	2898					1.7	

[a] Q branch maximum

[b] Band centre

[c] Ref. [69], similar values reported in Ref. [70]

[d] Ref. [71]

Table 6 Vibrational spectroscopy of ***9***

	Frequency/cm^{-1}			IR intensity/km × mol^{-1}	Raman activ./A^4 × AMU^{-1}
	Harmonic	Anharmonic	Ar matrix [a]	Harmonic	Harmonic
	CCSD(fc,T)	CCSD(T,fc) + B3LYP		CCSD,fc	B3LYP
ν_1 E	3132	2979		0.93	2.7×10^2
ν_2 A_1	3051	2976	2926	8.1	5.8×10^2
ν_3 A_1	2271	2228	2237, 2240	2.8×10^2	5.0×10^2
ν_4 E	1482	1448	1413	19	21
ν_5 A_1	1413	1395	1346	5.5	78
ν_6 E	1046	1023		3.6	2.3
ν_7 A_1	1020	1004	1005, 1001	54	1.8
ν_8 A_1	574	579	565	40	3.4
ν_9 E	406	405		0.82	2.1
ν_{10} E	140	144		1.1	4.2

[a] Ref. [64]

Table 7 ZPE-corrected singlet–triplet energetic separation (eV), as derived for the C_2H_3NS isomers using B3LYP/aug-cc-pVDZ and CCSD/cc-pVTZ calculations

Molecule	*B3LYP*	*CCSD*
1	2.3[a]	
2	2.7	2.8
3	3.1	3.6
4	2.4[a]	
5	2.9	3.1
6	1.5	1.6
7	2.1[b]	3.8
8	1.0	1.2
9	1.9	2.0
10	1.8[c]	2.0
11	1.8[c]	1.8
12	0.7	0.9
13	2.5	2.6
14	2.2	2.2

[a] Barrierless detachment of HS

[b] HNC-CH_2-S structure is adopted in the lowest triplet state

[c] The lowest triplet state structures of ***10*** and ***11*** are identical (planar)

dicted to have a sizable IR intensity. Its calculated position agrees well with the experimental [66] frequencies: 2789 (gas-phase) and 2791 cm^{-1} (argon matrix). This fits with the fundamental frequencies proposed by Zheng et al. [68].

4. The assignment of weak bands observed in the gas phase [65, 66] at 2823 and 2900 cm^{-1} or in solid argon [66] at 2818 and 2887 cm^{-1}, is not easy. These were interpreted in the gas phase as the overtones of CH_3 antisymmetric deformation modes ($2\nu_5$ or $2\nu_6$), possibly overlapping with the overtone of CH_3 antisymmetric deformation ($2\nu_7$) or the combination of CH_3 antisymmetric deformations ($\nu_6 + \nu_5$). Yet another explanation of the bands detected in that region may involve a combination of symmetric and antisymmetric CH_3 deformation modes, $\nu_6 + \nu_7$ and/or $\nu_5 + \nu_7$. Compared to prior assignments, the predicted frequencies of either $\nu_6 + \nu_7$ or $\nu_5 + \nu_7$ would be higher than the sum of the fundamentals.

Comparisons between the IR spectra of ***3*** and our results are not straightforward. Firstly, no obvious assignment of the band observed by Sullivan et al. [69] at 2112 (strong) and 2106 cm^{-1} (medium intensity) in gas and solid phases, respectively, can be given. Fundamental transitions are not expected there, while overtone and combination bands are predicted to be weak. The band most likely comes from impurities as it was not reported in another study [70].

Table 8 Energy (eV) and oscillator strength values for vertical transitions (ΔE_{vert} < 7.75 eV) from the ground electronic states of C_2H_3NS isomers, as derived using EOM-CCSD/cc-pVTZ

Isomer	State	ΔE_{vert}	f_{vert}
1	*A*	5.8	0.0001
	B	6.8	0.02
2	*A*	5.3	0
	B	5.5	0.004
	C	5.7	0.0001
	D	7.7	0.5
	E	7.7	0.004
3	*A*	5.5	0.0001
	B	7.0	0.002
	C	7.5	0.01
4	*A*	5.9	0.003
	B	7.1	0.02
5	*A*	4.8	0
	B	5.6	0.002
	C	6.0	0.01
	D	6.1	0.05
	E	7.4	0.004
6	*A*	2.8	0.0004
	B	4.6	0.07
	C	5.5	0.06
	D	6.1	0.05
	E	6.2	0.1
	F	7.1	0.003
	E	7.6	0.04
7	*A*	5.1	0.0007
	B	5.6	0.003
	C	5.9	0.01
	D	6.6	0.1
	E	7.4	0.001
8	*A*	2.1	0
	B	4.4	0.0007
	C	5.8	0.2
	D	6.6	0.007
	E	6.7	0.01
	F	7.3	0.01
	G	7.4	0.07
	H	7.6	0.02
9	*A*	4.8	0
	B	4.9	0.0002
	C	5.8	0.0009
	D	5.8	0.0009
	E	6.6	0.9
	F	6.7	0.0001
10	*A*	4.7	0.004
	B	5.9	0.005
	C	6.4	0.007
	D	6.6	0

Table 8 continued

Isomer	State	ΔE_{vert}	f_{vert}
	E	6.8	0.2
	F	7.2	0.1
	G	7.5	0.001
11	*A*	4.7	0.002
	B	5.9	0.008
	C	6.3	0.009
	D	6.9	0.1
	E	7.0	0.2
12	*A*	1.9	0.0004
	B	5.2	0.003
	C	5.8	0.02
	D	6.3	0.008
	E	7.0	0.04
	F	7.2	0.1
	G	7.2	0.03
	H	7.3	1.0
13	*A*	4.3	0.0001
	B	5.6	0.04
	C	5.8	0.001
	E	6.7	0.04
	F	6.7	0.0009
	G	7.3	0.02
	H	7.5	0.0003
	I	7.6	0.002
14	*A*	5.2	0.0009
	B	6.6	0.002
	C	7.4	0.02
	D	7.6	0.0001

3.2.3 Excited electronic states

Searches for both singlet (EOM-CCSD/cc-pVTZ and CIS/aug-cc-pVDZ) and triplet (B3LYP/aug-cc-pVDZ and CCSD/cc-pVTZ) excited states were performed. The results of the triplet search indicated that all ground electronic states are of singlet multiplicity. No minima corresponding to ***1*** or ***4*** could be found on the triplet potential energy surface. Instead, ***1*** and ***4*** converged to H_2C–CN + SH or H_2C–NC + SH, respectively. Table 7 lists singlet–triplet energy splittings predicted for the whole family of isomers.

Table 8 presents vertical electronic excitation energies for the most stable isomers. Strong UV absorption bands are predicted for species ***2***, ***7***, ***8***, ***9***, ***10***, ***11***, and ***12***. Differences between isomers ***2*** and ***3***, both featuring methyl groups and NCS structural units, are notable. The main UV absorption band of ***2*** is predicted to be far more intense ($f = 0.5$) than any of the bands predicted for ***3*** ($f < 0.01$, at least up to energies of 8.6 eV). This difference in intensities is rooted in the electronic structures of these molecules, differences between which can be seen in the results of charge distribution calculations given in Fig. 1. Only six of the discussed species, namely ***6***, ***8***, ***9***, ***10***, ***11***, and ***12***, have their first singlet excited states at less than 5 eV (248 nm).

Geometry optimizations using CIS/aug-cc-pVTZ, for selected excited singlet electronic states of the 14 most stable C_2H_3NS isomers, did not point to many significant changes in atomic arrangements that might occur as a result of excitation. We found that ***9*** dissociates in its first singlet excited state, reached through a vertical excitation energy of approximately 4.8 eV, into CH_3–CN and S. In the case of ***7***, electronic excitation breaks apart the bonds between sulfur and carbon atoms. For ***14*** an SNC ring can be created. The excitation of ***1*** to the second excited state is likely to yield the SH radical. This ease of photodecomposition may contribute to the reported low stability of ***1***. A similar process is to be expected for ***4***, but the breaking of C–S is accompanied by the creation of an H–C bond. As a result, S and $HCNCH_2$ may be created.

4 Summary and conclusions

Methyl isothiocyanate (CH_3–NCS, ***2***), methyl thiocyanate (CH_3–SCN, ***3***), and, surprisingly, mercaptoacetonitrile (HS–CH_2–CN, ***1***) are identified as the most thermodynamically stable molecules of C_2H_3NS stoichiometry. These three species are separated in energy by no more than 10 kJ/mol. Molecular constants for rotational, vibrational, and electronic spectroscopy were predicted for the 14 most stable isomers. Quantum chemical calculations suggest the susceptibility of mercaptoacetonitrile (***1***), mercaptoacetoisonitrile (HS–CH_2–NC, ***4***), and N-sulfide acetonitrile (CH_3–CNS, ***9***) to UV-induced decomposition.

Acknowledgments Authors acknowledge the financial support from the Polish National Science Centre, projects Nos. 2011/01/D/ST4/04345 and 2015/17/B/ST4/03875.

References

1. Sinclair MW, Fourikis N, Ribes JC, Robinson BJ, Brown RD, Godfrey PD (1973) Detection of interstellar thioformaldehyde. Austr J Phys 26(1):85–91. doi:10.1071/PH730085
2. Adande GR, Halfen DT, Ziurys LM, Quan D, Herbst E (2010) Observations of the [HNCS]/[HSCN] ratio in Sgr B2 AND

TMC-1: evidence for low-temperature gas-phase chemistry. Astrophys J 725(1):561–570. doi:10.1088/0004-637x/725/1/561
3. Halfen DT, Ziurys LM, Brünken S, Gottlieb CA, McCarthy MC, Thaddeus P (2009) Detection of a new interstellar molecule: thiocyanic acid Hscn. Astrophys J 702(2):L124–L127. doi:10.1088/0004-637x/702/2/l124
4. Frerking MA, Linke RA, Thaddeus P (1979) Interstellar isothiocyanic acid. Astrophys J 234:L143–L145. doi:10.1086/183126
5. Gronowski M, Kołos R (2014) A theoretical study on the interstellar synthesis of H_2NCS^+ and $HNCSH^+$ cations. Astrophys J 792(2):89. doi:10.1088/0004-637x/792/2/89
6. Wierzejewska M, Moc J (2003) Isomerization and dissociation of CHNS: quantum mechanical study. J Phys Chem A 107(50):11209–11216. doi:10.1021/jp030971b
7. Wierzejewska M, Mielke Z (2001) Photolysis of isothiocyanic acid HNCS in low-temperature matrices. Infrared detection of HSCN and HSNC isomers. Chem Phys Lett 349(3–4):227–234. doi:10.1016/s0009-2614(01)01180-0
8. Krupa J, Kosendiak I, Wierzejewska M (2015) New data on photochemistry of the interstellar molecule: HNCS. Identification of the S…HCN complex. Phys Chem Chem Phys 17(34):22431–22437. doi:10.1039/c5cp03663a
9. Smelt JH, Leistra M (1974) Conversion of metham-sodium to methyl isothiocyanate and basic data on the behaviour of methyl isothiocyanate in soil. Pestic Sci 5(4):401–407. doi:10.1002/ps.2780050405
10. van den Berg F (1993) Measured and computed concentrations of methyl isothiocyanate in the air around fumigated fields. Atmos Environ A General Top 27(1):63–71. doi:10.1016/0960-1686(93)90071-6
11. Woodrow JE, LePage JT, Miller GC, Hebert VR (2014) Determination of methyl isocyanate in outdoor residential air near metam-sodium soil fumigations. J Agric Food Chem 8921–8927. doi:10.1021/jf501696a
12. van den Berg F, Smelt JH, Boesten JJTI, Teunissen W (1999) Volatilization of methyl isothiocyanate from soil after application of metam-sodium with two techniques. J Environ Quality 28(3):918–928. doi:10.2134/jeq1999.00472425002800030024x
13. McDonald JR, Scherr VM, McGlynn SP (1969) Lower-energy electronic states of HNCS, NCS^-, and thiocyanate salts. J Chem Phys 51(5):1723–1731. doi:10.1063/1.1672256
14. Svátek E, Zahradník R, Kjær A, Sömme R, Stenhagen E, Palmstierna H (1959) Absorption spectra of alkyl isothiocyanates and N-alkyl monothiocarbamates. Acta Chem Scand 13:442–455. doi:10.3891/acta.chem.scand.13-0442
15. Northrup FJ, Sears TJ (1990) Photodissociation of RNCS and RSCN (R = H, CH3, C2H5) at 248 and 193 nm: CN product energy distributions. J Chem Phys 93(4):2346–2356. doi:10.1063/1.459014
16. Northrup FJ, Sears TJ (1990) Photodissociation of RNCS and RSCN (R = H, CH3, C2H5): evidence for an excited state isomerization and energy deposition in the NCS product. J Chem Phys 93(4):2337–2345. doi:10.1063/1.459013
17. D'Amario P, Di Stefano G, Lenzi M, Mele A (1972) Excited products in the photodissociation of methyl thiocyanate and isothiocyanate in the vacuum ultra-violet. J Chem Soc Faraday Trans Phys Chem Condens Phases 68:940. doi:10.1039/f19726800940
18. Nicholas JE, Amodio CA (1980) Mechanism of the decomposition of CH3SCN, CH3NCS and CH3CN in a radio-frequency pulse discharge. J Chem Soc Faraday Trans Phys Chem Condens Phases 76:1669–1676. doi:10.1039/f19807601669
19. Tokue I, Kobayashi K, Honda T, Ito Y (1990) Isothiocyanate radical produced by electron impact on methyl isothiocyanate and methyl thiocyanate. J Phys Chem 94(9):3485–3489. doi:10.1021/j100372a024
20. Wade EA, Pore JL, Osborn DL (2011) Infrared emission following photolysis of methylisothiocyanate and methylthiocyanate. J Phys Chem A 115(21):5319–5323. doi:10.1021/jp2000305
21. Li P, Ling Tan Y, Yip Fan W (2004) The CN and CS transient species in CH3SCN discharges. Chem Phys 302(1–3):171–177. doi:10.1016/j.chemphys.2004.04.005
22. Mollendal H, Samdal S, Guillemin JC (2016) Rotational spectrum, conformational composition, intramolecular hydrogen bonding, and quantum chemical calculations of mercaptoacetonitrile (HSCH2C identical withN), a compound of potential astrochemical interest. J Phys Chem A 120(12):1992–2001. doi:10.1021/acs.jpca.6b01600
23. Fu Z, X-m Pan, Z-s Li, C-C Sun, R-s Wang (2006) Theoretical study of the global potential energy surface of the [CH3, N, C, S] system in singlet and triplet states. Chem Phys Lett 430(1–3):13–20. doi:10.1016/j.cplett.2006.07.103
24. Koput J (1996) Ab initio potential energy surfaces for the large-amplitude motions of quasi-symmetric top molecules: CH3NCS and SiH3NCO. Chem Phys Lett 259(5–6):661–668. doi:10.1016/0009-2614(96)00820-2
25. Palmer MH, Nelson AD (2003) The structures of the azido-, isocyanato- and isothiocyanato- derivatives of methane and silane and their derivatives. A comparison of ab initio with experimental results. J Mol Struct 660(1–3):49–65. doi:10.1016/j.molstruc.2003.07.007
26. Saunders M (2004) Stochastic search for isomers on a quantum mechanical surface. J Comput Chem 25(5):621–626. doi:10.1002/jcc.10407
27. Gronowski M, Kołos R, Krełowski J (2013) A theoretical study on structure and spectroscopy of $C_4H_2^+$ isomers. Chem Phys Lett 582:56–59. doi:10.1016/j.cplett.2013.07.053
28. Gronowski M, Kołos R (2015) An ab initio study of structure, stability, and spectroscopic parameters of 5-atomic [C, C, H, N, S] isomers. J Mol Struct 1090:76–85. doi:10.1016/j.molstruc.2015.01.001
29. Becke AD (1993) Density-functional thermochemistry. III. The role of exact exchange. J Chem Phys 98(7):5648–5652. doi:10.1063/1.464913
30. Ditchfield R, Hehre WJ, Pople JA (1971) Self-consistent molecular-orbital methods. IX. An extended Gaussian-type basis for molecular-orbital studies of organic molecules. J Chem Phys 54(2):724–728. doi:10.1063/1.1674902
31. Hehre WJ, Ditchfield R, Pople JA (1972) Self-consistent molecular orbital methods. XII. Further extensions of Gaussian-type basis sets for use in molecular orbital studies of organic molecules. J Chem Phys 56(5):2257–2261. doi:10.1063/1.1677527
32. Harihara P, Pople JA (1974) Accuracy of Ah equilibrium geometries by single determinant molecular-orbital theory. Mol Phys 27(1):209–214. doi:10.1080/00268977400100171
33. Gordon MS (1980) The isomers of silacyclopropane. Chem Phys Lett 76(1):163–168. doi:10.1016/0009-2614(80)80628-2
34. Dunning TH (1989) Gaussian basis sets for use in correlated molecular calculations. I. The atoms boron through neon and hydrogen. J Chem Phys 90(2):1007. doi:10.1063/1.456153
35. Woon DE, Dunning TH (1993) Gaussian basis sets for use in correlated molecular calculations. III. The atoms aluminum through argon. J Chem Phys 98(2):1358–1371. doi:10.1063/1.464303
36. Barone V (2005) Anharmonic vibrational properties by a fully automated second-order perturbative approach. J Chem Phys 122(1):014108. doi:10.1063/1.1824881
37. Foster JP, Weinhold F (1980) Natural hybrid orbitals. J Am Chem Soc 102(24):7211–7218. doi:10.1021/ja00544a007
38. Reed AE, Weinstock RB, Weinhold F (1985) Natural population analysisa). J Chem Phys 83(2):735–746. doi:10.1063/1.449486

39. Reed AE, Weinhold F (1985) Natural localized molecular orbitals. J Chem Phys 83(4):1736–1740. doi:10.1063/1.449360
40. Čížek J (1969) On the use of the cluster expansion and the technique of diagrams in calculations of correlation effects in atoms and molecules. Adv Chem Phys Correl Effects Atoms Mol 14:35–89. doi:10.1002/9780470143599.ch2
41. Purvis GD, Bartlett RJ (1982) A full coupled-cluster singles and doubles model—the inclusion of disconnected triples. J Chem Phys 76(4):1910–1918. doi:10.1063/1.443164
42. Scuseria GE, Janssen CL, Schaefer HF (1988) An efficient reformulation of the closed-shell coupled cluster single and double excitation (Ccsd) equations. J Chem Phys 89(12):7382–7387. doi:10.1063/1.455269
43. Puzzarini C, Biczysko M, Barone V (2010) Accurate harmonic/anharmonic vibrational frequencies for open-shell systems: performances of the B3LYP/N07D model for semirigid free radicals benchmarked by CCSD(T) computations. J Chem Theory Comput 6(3):828–838. doi:10.1021/Ct900594h
44. Coupeaud A, Turowski M, Gronowski M, Pietri N, Couturier-Tamburelli I, Kołos R, Aycard JP (2008) C(5)N(−) anion and new carbenic isomers of cyanodiacetylene: a matrix isolation IR study. J Chem Phys 128(15):154303. doi:10.1063/1.2894875
45. Kołos R, Gronowski M, Dobrowolski JC (2009) Prospects for the detection of interstellar cyanovinylidene. Astrophys J 701(1):488–492. doi:10.1088/0004-637x/701/1/488
46. Gronowski M (2010) Teoria i eksperyment w badaniach spektroskopii wybranych nitryli o znaczeniu astrochemicznym oraz czasteczek pokrewnych. PhD Thesis, Institute of Physical Chemistry Polish Academy of Sciences, Poland, Warszawa
47. Gronowski M, Kołos R (2006) Isomers of cyanodiacetylene: theoretical structures and IR spectra. Chem Phys Lett 428(4–6):245–248. doi:10.1016/j.cplett.2006.07.041
48. Gronowski M, Kołos R (2007) Isomers of cyanodiacetylene: predictions for the rotational, infrared and Raman spectroscopy. J Mol Struct 834:102–108. doi:10.1016/j.molstruc.2006.10.003
49. Frisch MJ, Trucks GW, Schlegel HB, Scuseria GE, Robb MA, Cheeseman JR, Scalmani G, Barone V, Mennucci B, Petersson GA, Nakatsuji H, Caricato M, Li X, Hratchian HP, Izmaylov AF, Bloino J, Zheng G, Sonnenberg JL, Hada M, Ehara M, Toyota K, Fukuda R, Hasegawa J, Ishida M, Nakajima T, Honda Y, Kitao O, Nakai H, Vreven T, Montgomery JA Jr, Peralta JE, Ogliaro F, Bearpark MJ, Heyd J, Brothers EN, Kudin KN, Staroverov VN, Kobayashi R, Normand J, Raghavachari K, Rendell AP, Burant JC, Iyengar SS, Tomasi J, Cossi M, Rega N, Millam NJ, Klene M, Knox JE, Cross JB, Bakken V, Adamo C, Jaramillo J, Gomperts R, Stratmann RE, Yazyev O, Austin AJ, Cammi R, Pomelli C, Ochterski JW, Martin RL, Morokuma K, Zakrzewski VG, Voth GA, Salvador P, Dannenberg JJ, Dapprich S, Daniels AD, Farkas Ãd, Foresman JB, Ortiz JV, Cioslowski J, Fox DJ (2009) Gaussian 09. Gaussian Inc., Wallingford
50. Gauss J, Tajti A, Kallay M, Stanton JF, Szalay PG (2006) Analytic calculation of the diagonal Born-Oppenheimer correction within configuration-interaction and coupled-cluster theory. J Chem Phys 125(14):144111. doi:10.1063/1.2356465
51. Cowan RD, Griffin DC (1976) Approximate relativistic corrections to atomic radial wave-functions. J Opt Soc Am 66(10):1010–1014. doi:10.1364/Josa.66.001010
52. Klopper W (1997) Simple recipe for implementing computation of first-order relativistic corrections to electron correlation energies in framework of direct perturbation theory. J Comput Chem 18(1):20–27. doi:10.1002/(Sici)1096-987x(19970115)18:1<20:Aid-Jcc3>3.0.Co;2-1
53. Halkier A, Helgaker T, Jorgensen P, Klopper W, Koch H, Olsen J, Wilson AK (1998) Basis-set convergence in correlated calculations on Ne, N_2, and H_2O. Chem Phys Lett 286(3–4):243–252. doi:10.1016/S0009-2614(98)00111-0
54. Helgaker T, Klopper W, Koch H, Noga J (1997) Basis-set convergence of correlated calculations on water. J Chem Phys 106(23):9639–9646. doi:10.1063/1.473863
55. Stanton JF, Gauss J, Harding ME, Szalay PG CFOUR, Coupled-cluster techniques for computational chemistry, a quantum-chemical program package. University of Texas and Universitaet Mainz. http://www.cfour.de,
56. Bloino J, Biczysko M, Barone V (2012) General perturbative approach for spectroscopy, thermodynamics, and kinetics: methodological background and benchmark studies. J Chem Theory Comput 8(3):1015–1036. doi:10.1021/ct200814m
57. Reed MG, Zhang DY (2001) Thionitroso or thiazyl? Density functional studies of relative stabilities between the two structural isomers. J Mol Struct Theochem 548(1–3):107–112. doi:10.1016/s0166-1280(01)00514-0
58. Kuznetsova TA, Istomina NV, Krivdin LB (2000) Russ J Org Chem 36:638–644
59. Helgaker T, Jorgensen P, Olsen J (2004) Molecular electronic-structure theory. Wiley, Toronto
60. Gaumont AC, Wazneh L, Denis JM (1991) Thiocyanohydrins, a new class of compounds, precursors of unstabilized thiocarbonyl derivatives. Tetrahedron 47(27):4927–4940. doi:10.1016/s0040-4020(01)80958-3
61. Mathias E, Shimanski M (1981) Synthesis of mercaptoacetonitrile under mild conditions. J Chem Soc Chem Commun 11:569. doi:10.1039/c39810000569
62. Lett RG (1967) Microwave spectrum, barrier to internal rotation, 14 N nuclear quadrupole interaction, and normal-coordinate analysis in methylisocyanate, methylisothiocyanate, and methylthiocyanate. J Chem Phys 47(11):4730. doi:10.1063/1.1701692
63. Nakagawa S, Takahashi S, Kojima T, Lin CC (1965) Microwave spectrum and internal rotation of methylthiocyanate. J Chem Phys 43(10):3583. doi:10.1063/1.1696523
64. Krebsz M, Hajgató B, Bazsó G, Tarczay G, Pasinszki T (2010) Structure, stability, and generation of CH3CNS. Aust J Chem 63(12):1686. doi:10.1071/ch10303
65. Durig JR, Sullivan JF, Heusel HL, Cradock S (1983) Infrared and Raman spectra and normal coordinate calculations for methylisothiocyanate. J Mol Struct 100:241–257. doi:10.1016/0022-2860(83)90095-9
66. Durig JR, Sullivan JF, Durig DT, Cradock S (1985) Infrared spectra of some matrix isolated organoisothiocyanate molecules. Can J Chem 63(7):2000–2006. doi:10.1139/v85-331
67. Kniseley RN, Hirschmann RP, Fassel VA (1967) The infrared spectra of alkyl isothiocyanates. Spectrochim Acta A 23(1):109–127. doi:10.1016/0584-8539(67)80212-5
68. Zheng C, Guirgis GA, Deeb H, Durig JR (2007) On the structural parameters and vibrational spectra of CH3NCS, SiH3NCS and GeH3NCS. J Mol Struct 829(1–3):88–110. doi:10.1016/j.molstruc.2006.06.011
69. Sullivan JF, Heusel HL, Durig JR (1984) Infrared and raman spectra of methyl thiocyanate and conformations of some alkyl thiocyanates and isothiocyanates. J Mol Struct 115:391–396. doi:10.1016/0022-2860(84)80096-4
70. Moritz AG (1966) Infra-red and Raman spectra of methyl thiocyanate and methyl-d3 thiocyanate. Spectrochim Acta 22(6):1021–1028. doi:10.1016/0371-1951(66)80191-1
71. Fateley WG, Miller FA (1961) Torsional frequencies in the far infrared—I. Spectrochim Acta 17(8):857–868. doi:10.1016/0371-1951(61)80153-7